RSC Pharmaceutics

ROYAL SOCIETY OF CHEMISTRY

PAPER

View Article Online
View Journal | View Issue

Cite this: *RSC Pharm.*, 2024, **1**, 716

Effect of amorphous chrysin loading in hydrophobically modified Pluronic F68 nanomicelles on its anticancer activity, stability and oral bioavailability

Harihar Narayan,[a] Ashok Kumar Jangid,[b] Jiten R. Sharma,[c] Ankita Kishore,[a] Alok Kumar Mahor,[a] Umesh C. S. Yadav,[c] Hitesh Kulhari *[b] and Prem Prakash Singh*[a]

Received 12th March 2024,
Accepted 26th April 2024

DOI: 10.1039/d4pm00074a

rsc.li/RSCPharma

Designing a potential polymer-based drug delivery carrier is of great significance for enhancing the anticancer effectiveness and oral delivery of hydrophobic phytodrugs. Chrysin (CRY) is a potential anticancer phytomolecule; however, its utilization for further applications is restricted due to its low aqueous solubility and poor bioavailability. Here, a biocompatible polymer, *i.e.* Pluronic F68 modified with stearic acid (F68–SA) was used for the fabrication of chrysin-loaded nanomicelles (CNMs). The fabricated CNMs comprised particles of 142.7 nm size with a spherical shape, amorphous nature, and a drug encapsulation efficiency of 37.06%. The incorporation of a hydrophobic segment into Pluronic F68 significantly enhanced the sustained drug release profile and stability. The CNMs effectively enhanced the anticancer effect against human lung A549 cancer cells, as confirmed by MTT, AO/EB, and cellular uptake assays. Moreover, the fabricated CNMs demonstrated a higher plasma chrysin concentration–time (C_{max}) profile compared to a chrysin suspension. The AUC_{0-t} of the CNMs was also 5.6 times higher than that of the CRY suspension. These results indicate that the bioavailability of chrysin was significantly improved due to faster and enhanced absorption after administration as a nanomicelle formulation.

1. Introduction

Chrysin (CRY), alternatively recognized as a 5,7-dihydroxyflavone-based bioactive molecule, has the molecular formula $C_{15}H_{10}O_4$.[1] It is mainly extracted from various sources such as trees, honey, and propolis. Chrysin exhibits diverse pharmacological activities, including potent antimicrobial, anti-inflammatory, anticancer, and antioxidant properties.[2,3] However, the use of chrysin in further clinical trials is restricted due to its potential cytotoxicity and notable side effects. In previous reports, it has been observed that a specific dose of chrysin can mitigate the chemotherapeutic toxicity associated with *cis*-diamine dichloroplatinum(II).[4] In addition, due to its capability to induce apoptosis and more effective inhibition of cell proliferation compared to other flavone molecules, chrysin also exhibits heightened immunosuppressive activity.[5] Despite the widely documented health benefits of chrysin, its utilization for cancer treatment is still not fully optimized. The limitation of chrysin occurs from its poor oral bioaccessibility and bioavailability, poor solubility in gastrointestinal fluids, low permeability across epithelial cells and molecular transformations within the gastrointestinal tract.[6]

Encapsulation techniques involve capping active drug molecules within wall-based materials. The encapsulation method, especially micellization, is used to safely deliver bioactive drugs at the site of action, and is also more susceptible to protection from the harsh gastric environment.[7] The micelles are developed through the assembly of amphiphilic polymers containing both hydrophilic and hydrophobic segments, with the inner hydrophobic segment enabling the loading of active drug molecules.[8] These micelles exhibit excellent biocompatibility, stability, and the ability to modulate the surface periphery for drug delivery at the targeted site of action.[9–11] Pluronics are a revolutionary class of linear polymers with amphiphilic features. Pluronic F68 is a non-ionic, non-toxic, US-FDA-approved polymer that makes it an excellent drug delivery system.[12,13] In recent years, Pluronic F68 has been thoroughly investigated for its capacity to dissolve hydrophobic medications. However, it is subject to certain constraints such as

[a]*Institute of Pharmacy, Bundelkhand University, Jhansi 284128, India. E-mail: premvrajput@gmail.com*
[b]*School of Nano Sciences, Central University of Gujarat, Sector 30, Gandhinagar 382030, India. E-mail: hitesh.kulhari@cug.ac.in*
[c]*Special Centre for Molecular Medicine, Jawaharlal Nehru University, New Delhi 110067, India*

diminished drug loading capability and premature breakdown upon dilution in biological fluids, leading to diminished stability and suboptimal bioavailability.[14] These challenges can be overcome through Pluronic F68 modification instead of relying solely on singular Pluronic micelles for micelle development.[15–17]

In our previous reports, we utilized Pluronic F68 modified with stearic acid (F68–SA) and inulin for the development of nanomicelles aimed at enhancing the oral bioavailability of hydrophobic drugs.[18–20] The significant impact on hydrophobic drug solubilization, anticancer activity, and pharmacokinetics studies revealed the specific contribution of Pluronic F68 to nanomicelle development. Herein, the utilization of Pluronic F68 modified with stearic acid (F68–SA) was demonstrated in the development of nanomicelles for enhancing therapeutic efficacy and oral bioavailability of CRY. The fabricated nanomicelles were successfully characterized by DLS and TEM analyses. The fabricated nanomicelles effectively inhibited the growth of human A549 lung cancer cells, as confirmed by cell viability, induction of apoptosis, and cellular uptake assays. Furthermore, chrysin-loaded nanomicelles (CNMs) were orally administered to SD rats, and their pharmacokinetics (PK) parameters were evaluated. The observed anticancer results and PK parameters clearly demonstrate the advantages of fabricated nanomicelles over bolus chrysin administration.

2. Materials and methods

2.1 Materials

Chrysin (CRY), stearic acid (SA), *N*-(3-(dimethylamino)propyl)-*N*′-ethylcarbodiimide (EDC), 1-hydroxybenzotriazole hydrate (HOBt), pyrene, dimethyl sulfoxide (DMSO), triethylamine (TEA) and dialysis tubing (molecular weight cutoff 12 000–14 000) were obtained from Sigma-Aldrich (St. Louis, MO, USA). Pluronic F68 was obtained as a gift sample from BASF Corporation (New Jersey, USA). Human lung adenocarcinoma A549 cells were procured from the American-type culture collection (ATCC, Manassas, USA). The cells were preserved in fetal bovine serum (10%, Gibco) in RPMI medium, further supplemented with penicillin–streptomycin antibiotic solution (1%, Gibco). A humidified incubator with 5% CO_2 at 37 °C was used for regular maintenance of the cultures.

2.2 Synthesis and characterization of the Pluronic F68–SA conjugate (PF68–SA)

The PF68–SA conjugate was synthesized following our previously established method.[20,21]

2.3 Preparation of drug-loaded nanomicelles

Nanomicelles loaded with CRY were fabricated using the method previously reported.[21] Briefly, Pluronic F8 or SA-modified Pluronic F68 (F68–SA) and CRY with different drug/polymer ratios, namely 12, 6 and 3%, were dissolved in 2 mL of methanol and stirred for 30 min and then the methanol was evaporated using a Rotavapor. After the formation of a thin layer of drug/polymer mixture, the layer was rehydrated with 5 mL of DW and stirred for 1 h at 500 rpm. After this, the obtained formulation was filtered through 0.22 μm filter paper and the filtrate (CNMs) was collected and used for further studies. The lyophilized CNMs were analyzed using NMR, DSC and XRD. No-drug-containing or blank nanomicelles (BNMs) were also prepared using the above-mentioned method. The amount of CRY loaded into the polymer (CNMs) was calculated as follows:

$$\%\,\text{Encapsulation efficiency} = \left(\frac{\text{Amount of CRY present in nanomicelles}}{\text{Amount of CRY added to the polymer}}\right) \times 100$$

$$\%\,\text{Drug loading efficiency} = \left(\frac{\text{Amount of CRY present in nanomicelles}}{\text{Amount of CRY loaded nanomicelles}}\right) \times 100.$$

2.4 Characterization of chrysin nanomicelles

The particle size and polydispersity index of the nanomicelles were assessed using the dynamic light scattering technique employing a Zetasizer Nano ZS 90 (Malvern Instruments, UK). The analysis was conducted at 25 °C with a backscattering angle of 173°. The morphology of the prepared CNMs was examined by transmission electron microscopy (TEM) using a JEM-2100 instrument (JEOL, Tokyo, Japan). For ^{1}H-NMR analysis, pure CRY powder and lyophilized BNMs or CNMs were dissolved in a deuterated solvent and scanned using a Bruker 500 MHz Ultra Shield Plus NMR instrument. X-ray diffraction patterns of pure CRY powder and lyophilized BNMs or CNMs were acquired using an X-ray diffractometer (D8 Advance, Bruker, Germany) equipped with a Cu-Kα X-ray radiation source. The instrumental parameters were set at 40 kV and 30 mA, with the diffraction angle (2θ) measured in the range of 5° to 80°. DSC scans of pure CRY powder and lyophilized BNMs or CNMs were recorded using a DSC-4000 instrument (PerkinElmer). The samples were subjected to scanning from 30 to 350 °C at a rate of 10 °C min^{-1} under a nitrogen environment.

2.5 *In vitro* drug release and stability study

The CRY release profile was studied in pH 1.2 and pH 6.8 buffers, as reported previously. Briefly, a 1 mL formulation equivalent to 2 mg of CRY was transferred to dialysis tubing (MWCO 1000) and then it was placed in 40 mL of pH 1.2 release media for 2 h and then transferred into another 40 mL of pH 6.8 release media. During the study, the temperature of the media was maintained at 37 ± 0.5 °C. At various time intervals, a two mL aliquot of the release media was withdrawn and replaced with an equal volume of fresh medium to ensure sink conditions and maintain a constant volume of external release medium. The samples were then analysed for their CRY content using UV-visible spectroscopy. The colloidal stability of the CNMs was preserved at room temperature and refriger-

ated temperature for up to 96 h. The stability was assessed by measuring the CRY content after storing the formulation in a colloidal state at both room temperature and refrigerated temperature.

2.6 MTT cell viability assay

Almost 1×10^4 A549 cells were seeded in 96-well plates and allowed to adhere. Subsequently, the cells were exposed to plain CRY, BNMs, and CNMs (2.5, 5, 10, 20, 40, and 60 μg mL^{-1}) for 24 and 48 h. After treatment at different time points, the media of the wells were decanted followed by the addition of MTT (5 mg mL^{-1}) prepared using phosphate-buffered saline (PBS). The plates were then incubated in a CO_2 incubator for 4 h. After the incubation period with the MTT reagent, the formazan crystals that formed at the bottom of the wells were dissolved in DMSO (150 μL per well). The plates were then analyzed using a multimode reader (BioTek, Synergy Hybrid Reader H1, Winooski, VT) at 570 nm.

2.7 Acridine orange and ethidium bromide staining

To determine the mode of cell death, dual staining with acridine orange and ethidium bromide was conducted. First, approximately 3×10^4 cells per well were plated in a 24-well plate. After reaching the desired confluency and growth, the cells were incubated with CRY, BNMs, and CNMs for 24 and 48 h. Following incubation, the cells were harvested using a trypsin EDTA solution, pelleted down, and subsequently washed with 1× PBS buffer. The cell suspension was then stained with acridine orange (1 mg mL^{-1} in PBS buffer) and ethidium bromide (1 mg mL^{-1} in PBS buffer). A 10 μL sample was mounted on a glass slide and observed under a fluorescence microscope (Zeiss, Germany) equipped with a digital camera, enabling the assessment of cell death-associated phenotypes and acquisition of images. Magnification was set at 200×.

2.8 Clonogenic assay

To assess the efficacy of synthesized formulations on the colony formation potential and *in vitro* antitumor activity, a clonogenic assay was performed. Roughly 500 cells per well were seeded in a 6-well plate and allowed to adhere and acquire morphology over a 24 h period. Subsequently, the cells were incubated with CRY, BNMs, and CNMs, and then returned to the CO_2 incubator for 7 days without disturbance. At the end of the incubation time, the plates were analyzed for the colonies formed. The medium in the wells was decanted, and the cells were washed using 1× PBS followed by fixation in 95 : 5 ethanol (100%) and glacial acetic acid solution for 20 minutes. The cells were again washed in 1× PBS to remove the fixing solution and incubated in crystal violet–ethanol solution (0.2% crystal violet in 2% ethanol) for 30 minutes. After staining of the colonies, the plates were subjected to perfusion washing with distilled water until the water ran clear from the wells. The stained colonies were photographed, followed by dye extraction using the dye extraction solution (0.5% sodium dodecyl sulfate in 50% ethanol). The extracted dye was assessed at 570 nm on a multiplate reader (Synergy, BioTek), and the relative colony formation in the treatment groups compared to the untreated control was documented.

2.9 Cellular uptake assay

To perform the cellular uptake studies, a fluorochrome, coumarin 6 (C6), and C6-loaded nanomicelles (C6NMs) were formulated separately. About 8×10^4 human lung adenocarcinoma cells were plated in 35 mm dishes followed by exposure to C6 and C6NMs at 0.5, 1, 4, and 8 h time intervals. The plates were subjected to 1× PBS washing to get rid of background noise due to the unbound dye. The fluorescence intensity was evaluated, and images were captured using a Zeiss fluorescence microscope at a magnification of 200×.

2.10 Pharmacokinetics study

All animal procedures were performed in accordance with the Guidelines for Care and Use of Laboratory Animals of Bundelkhand University and approved by the Animal Ethics Committee of Bundelkhand University, Jhansi. Twelve rats were randomly divided into two groups ($n = 6$) and orally administered with the CRY suspension and CNMs at a single dose of 50 mg kg^{-1}. Blood samples (0.3 mL) were collected in heparinized tubes at 0.5, 1, 1.5, 2, 4, 8, and 12 h post-administration. The blood samples were then centrifuged at 5000 rpm for 10 min, and the supernatants were stored at −80 °C. The CRY content in the samples was analysed using an HPLC system equipped with a UV detector and a C18 column (250 × 4.6 mm, 5 μm). The mobile phase consisted of acetonitrile (62%) and water acidified with 0.1 v/v orthophosphoric acid (38%). The flow rate of the mobile phase was maintained at 1 mL min^{-1}, and the column temperature was set at 25 ± 2 °C. Each sample was injected with a volume of 20 μL, and analysis was performed at 266 nm. Pharmacokinetics parameters were calculated using PK Solver software.

2.11 Statistical analysis

All results were graphed using Origin 8.5 software (Origin Lab Corporation), with NMR results plotted using MestReNova 6.0.2-5475 software. Statistical analysis was conducted using GraphPad Prism 8.0.2 (GraphPad Software Inc.). Student's *t*-test was employed for comparing two groups, and results were expressed as mean ± SEM. A *p*-value of <0.05 was considered statistically significant. Pharmacokinetics parameters were determined using PK Solver software.

3. Results and discussion

3.1 Development of chrysin nanomicelles

The development of advanced nanomicelles is important to the fields of pharmaceutical science and nanotechnology since these self-assembling nanoscale structures can be used in a variety of medical, cosmetic, and materials science applications and as efficient carriers for drug delivery.[22,23] The nanomicelles exhibit unique properties including (1) the

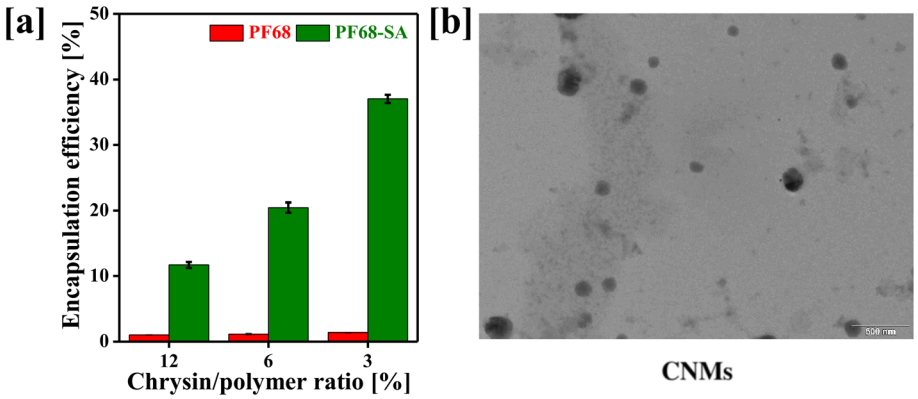

Fig. 1 (a) Percentage encapsulation efficiency (% EE) of different chrysin/polymer ratios [values represent mean ± SD (n = 3)], and (b) TEM image of the chrysin-loaded PF68–SA biomaterial nanomicelles.

amphiphilic nature of the polymer, (2) micelle structure and (3) stability.[24,25] As compared to surfactant-based micelles, block-*co*-polymers form more stable nanomicelles, lower the CMC and show slower dissociation rates. In the last few years, polymer-based nanomicelles have found potential therapeutic applications due to their potential ability to enhance the solubility of hydrophobic drugs, leading to improved intestinal permeability, prolonged circulation in the bloodstream and substantial accumulation in tumor tissues, making them valuable for targeting cancerous growths.[26–29]

Considering the advantages of block copolymers, we have developed chrysin (CRY)-loaded nanomicelles (CNMs) using Pluronic F68 for the oral delivery of CRY. However, stearic acid was conjugated to Pluronic F68 to increase hydrophobicity to enhance the loading of hydrophobic molecules. The CRY was encapsulated in the core of the PF68–SA biomaterial. Fig. 1a demonstrates the percentage of CRY encapsulated in the biomaterial at different drug-to-polymer ratios (12%, 6%, and 3%). The percentage of CRY encapsulation in F68 was found to be 1.03% ± 0.06%, 1.13% ± 0.11%, and 1.35% ± 0.05% for 12%, 6%, and 3% of chrysin/F68, respectively. Additionally, the percentage CRY encapsulation in the F68–SA biomaterial was 11.69% ± 0.46%, 20.44% ± 0.77%, and 37.06% ± 0.62% for the 12%, 6%, and 3% chrysin/F68–SA biomaterial ratio, respectively. Thus, the drug-loading efficiency was 0.95%, 3.29% and 11% for the 12%, 6%, and 3% chrysin/F68–SA biomaterial ratio, respectively.

Plain PF68 showed lower CRY encapsulation compared to the PF68–SA biomaterial. These results suggest that the insertion of a hydrophobic chain into PF68 terminals significantly enhances the solubility of poorly water-soluble CRY. This is achieved by forming double-folded nanomicelles through the amphiphilic PF68–SA biomaterial, where the PPO segments and SA help solubilize CRY in the core of nanomicelles with a nanosized spherical shape (Fig. 1b). This approach is particularly beneficial for drug delivery and enhancing oral bioavailability, as it efficiently encapsulates the drug within the polymer segments. Therefore, the incorporation of a hydrophobic linker into the PF68 polymer is a crucial strategy for overcoming challenges associated with most hydrophobic molecules.[30,31] Nanomicelles based on the PF68–SA biomaterial are nano-sized structures formed by the self-assembly of hydrophilic PEO and hydrophobic PPO/SA segments in an aqueous solution.[32] The size of the fabricated CNMs was determined using DLS analysis. Typically, the size of the CNMs is characterized in terms of their hydrodynamic diameter, which was measured at 142.7 nm, with a PDI of 0.259 and a zeta potential of −15.7 mV (Table 1).

Table 1 Particle sizes, PDIs and zeta potentials of blank and CRY-loaded nanomicelles. Values represent mean ± SD (n = 3)

Sample	Particle size (nm)	PDI	Zeta potential (mV)
BNMs	189.55 ± 8.83	0.285 ± 0.035	−9.20 ± 3.45
CNMs	142.73 ± 7.56	0.259 ± 0.114	−15.7 ± 4.72

BNMs: blank F68–SA nanomicelles; CNMs: chrysin-loaded F68–SA biomaterial nanomicelles.

3.2 Solid-state characterization of nanomicelles

The solid-state properties of drugs and drug-loaded nanomicelles, including their crystalline form, can significantly influence their solubility, release behaviour, and oral bioavailability.[33–35] The amorphous nature of the encapsulated hydrophobic drugs tends to lead to high solubility compared to that of bolus drugs.[36] The physical nature of the drug present in the core of the polymer was evaluated by NMR, DSC, and XRD analyses. As demonstrated in Fig. 2a, the ^{1}H-NMR spectra of pure CRY molecules and CNMs confirmed the presence of CRY in the core of the PF68–SA conjugate. Pure CRY shows characteristic peaks at 3.37, 6.24, 6.55, 7.01, 7.58–7.65, 8.08–8.10, 10.97 and 12.85 ppm. Similarly, the CNMs show both PF68–SA and CRY peaks at 1.04, 1.24, 3.37, 3.57, 5.78, 5.99, 6.24, 6.55, 7.01, 7.59–7.62, 8.10, 10.97 and 12.85 ppm. This analysis confirmed the presence of CRY within the core of the PF68–SA conjugate. Pure CRY exhibited characteristic peaks at specific chemical shifts, while CNMs displayed peaks corresponding to both PF68–SA and CRY. The

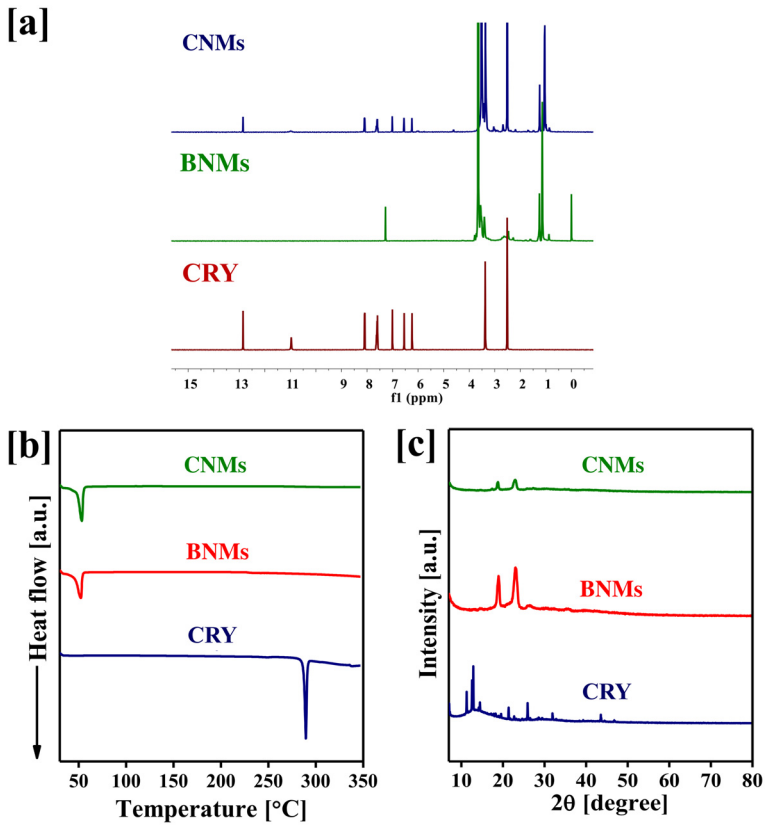

Fig. 2 (a) Proton-NMR spectra of pure chrysin (CRY), blank F68–SA nanomicelles (BNMs) and chrysin-loaded F68–SA biomaterial nanomicelles (CNMs), (b) the DSC thermograms of CRY, BNMs and CNM, and (c) XRD patterns of CRY, BNMs and CNMs.

coexistence of these peaks in the CNM spectra provides conclusive evidence of the presence of CRY in the nanomicellar system.

Furthermore, we subjected CNMs to DSC and XRD measurements to investigate their crystalline properties. As depicted in Fig. 2b, pure CRY exhibited an endothermic peak at 288 °C, indicative of its melting point. However, this peak was absent in the CNM spectrum, suggesting a transformation in the drug's physical state during the nanomicelle formation process. Additionally, we assessed the crystallinity of the encapsulated CRY through XRD measurements. Pure CRY exhibited distinct sharp crystalline XRD signals at specific angles (2θ). In contrast, the XRD spectra of CNMs did not show these peaks, as seen in Fig. 2c. These results suggest that the encapsulated drug within the nanomicelles exists in an amorphous state, which can be advantageous for the oral delivery of the nanomicelles.

3.3 *In vitro* drug release profile and stability of nanomicelles

Less water-soluble drugs can often be made more soluble and bioavailable when administered orally in the form of nanomicelles.[37] The drug release profile of orally delivered nanomicelles is crucial for determining the release pattern in the gastrointestinal (GI) tract, which ultimately influences absorption into the systemic bloodstream.[38] Therefore, designing nanomicelles for oral delivery requires an understanding of the release profile to ensure the desired therapeutic effects, particularly for cancer-cell killing. In other words, modifying the polymers with hydrophobic moieties can significantly affect the drug release profile in different pH buffers.[39,40] In our current study, we have assessed the drug release profile of the designed CNMs in two different release media at pH 1.2 and pH 6.8. For systematic comparison, we prepared a bolus CRY suspension and CRY-loaded F68 nanomicelles. It was observed that 99% of CRY was released from the CRY suspension within 1 hour of incubation, and over 90% of CRY was released within 2 hours from F68 nanomicelles under pH 1.2 buffer conditions. Additionally, approximately 50% of CRY was released from the CNM formulation after 2 hours in pH 1.2 buffer, with the remaining 50% being released in a phosphate buffer medium (as shown in Fig. 3a). As a result, CNMs exhibited a more favourable release profile compared to the CRY suspension and CRY-F68 nanomicelles. These findings suggest that the incorporation of stearic acid into the F68 polymer efficiently encapsulated CRY within the core of the nanomicelles during micelle formation, resulting in a sustained drug release profile.

The stability of nanomicelles is an important parameter in the fabrication of new formulations, as it significantly impacts the efficacy and safety profile of the drug for further appli-

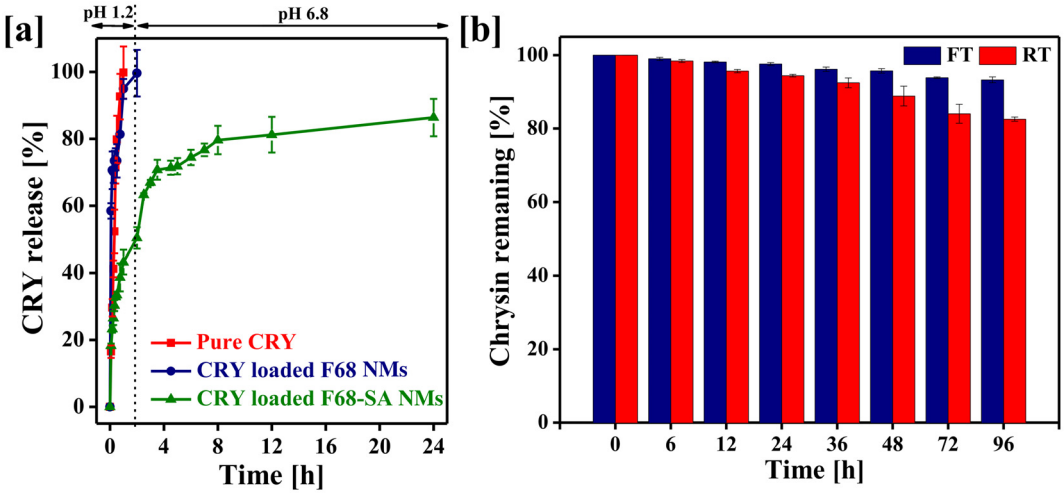

Fig. 3 (a) Chrysin release profile of the pure chrysin suspension (CRY), chrysin-loaded F68 nanomicelles and chrysin-loaded F68–SA conjugate nanomicelles (CNMs) in pH 1.2 and pH 6.8 media, and (b) the percentage of CRY remaining in nanomicelles after storage at room temperature (RT) and freezing temperature (FT). Values represent mean ± SD (n = 3).

cation. To ensure the stability of CNMs, we conducted stability tests by storing CNMs under freezing and room temperature (RT) conditions for up to 96 hours. Fig. 3b illustrates the percentage of CRY remaining in CNMs after storage under these conditions. The results showed that over 90% of CRY remained stable under freezing conditions and over 80% at room temperature within nanomicelles. These findings indicate that the drug remained highly stable after encapsulation in PF68–SA, both at freezing temperature and room temperature.

3.4 Chrysin-loaded nanomicelles reduce the viability of A549 adenocarcinoma cells

The role of nanomicelles as delivery vehicle for the anticancer agents has garnered significant attention in the field of cancer treatment.[41] These nanoscale structures, based on amphiphilic polymers, offer various advantages for delivering hydrophobic anticancer compounds. The choice of polymeric biomaterials to encapsulate the drug can significantly influence the success of nanomicelles in killing cancer cells.[42] CRY is a natural flavonoid found in various plants, and it exhibits potential anticancer properties against various types of cancer cells.[43,44] CRY exhibits the ability to inhibit the growth and proliferation of lung cancer cells. Here, we evaluated the anticancer effects of CRY and designed CNMs against human lung A549 cancer cells.

To evaluate the impact of CRY and CNMs on the viability of A549 adenocarcinoma cells, we conducted the MTT cell viability assay after incubating the cells with various concentrations of CRY or CNMs. As shown in Fig. 4a and b, CNMs exhibited significant cytotoxicity towards the A549 cells at both 24 and 48 hours across all tested doses ($p < 0.05$ to $p < 0.0001$). The cell viability of A549 cells, following treatment with CNMs, was 86% at a concentration of 2.5 μg mL^{-1} and decreased to 84.4%, 83%, 74.5%, 40.3%, and 35% after 24 hours. Similarly, the cell viability varied from 76.7% at 2.5 μg mL^{-1} to 72.1%, 73.1%, 62.3%, 18.5%, and 14.3% after 48 hours. Furthermore, when compared to bolus CRY, CNMs exhibited greater cytotoxicity toward A549 cells ($p < 0.5$ to $p < 0.0001$). The enhanced anticancer profile of CRY in nanomicelle form may be attributed to its ability to inhibit the glutathione-*S*-transferase/glutathione system, which plays a role in inducing drug resistance in A549 cells. These findings suggest that CNMs, as drug delivery systems, hold promise for improving the anticancer efficacy of CRY, particularly against lung cancer cells, by addressing drug resistance mechanisms.

Furthermore, the evaluation of anticancer effects was corroborated using the acridine orange and ethidium bromide dual staining assay, which allowed us to assess the different cell death phenotypes. A549 cells treated with CRY at concentrations of 10 μg mL^{-1} and 40 μg mL^{-1}, as well as with CNMs at the same concentrations, exhibited signs of apoptosis after 24 hours of incubation. In the group of cells exposed to CNMs at a concentration of 10 μg mL^{-1}, there were more early apoptotic cells and late apoptotic cells that were stained orange. At a higher concentration of CNMs (40 μg mL^{-1}), more cells showed late apoptosis, and some displayed necrotic characteristics, appearing red with fragmented nuclei. Conversely, cells treated with CRY showed only early apoptotic features, with a condensed nucleus (as illustrated in Fig. 4c). Similarly, after 48 hours, a higher proportion of cells exhibited late apoptotic characteristics in the CRY-treated group, while orange-stained cells were predominant in the group treated with a higher dose of CNMs (40 μg mL^{-1}).

3.5 Chrysin nanomicelles showed long-term cytotoxicity

The long-term cytotoxicity of the designed CNMs was assessed using the clonogenic assay. The treatment doses for CRY or CNMs were chosen based on the cell viability assay (as mentioned in Fig. 4a and b). After incubating A549 cells with CRY, BNMs and CNMs, we observed that CNM (10 μg mL^{-1})-treated

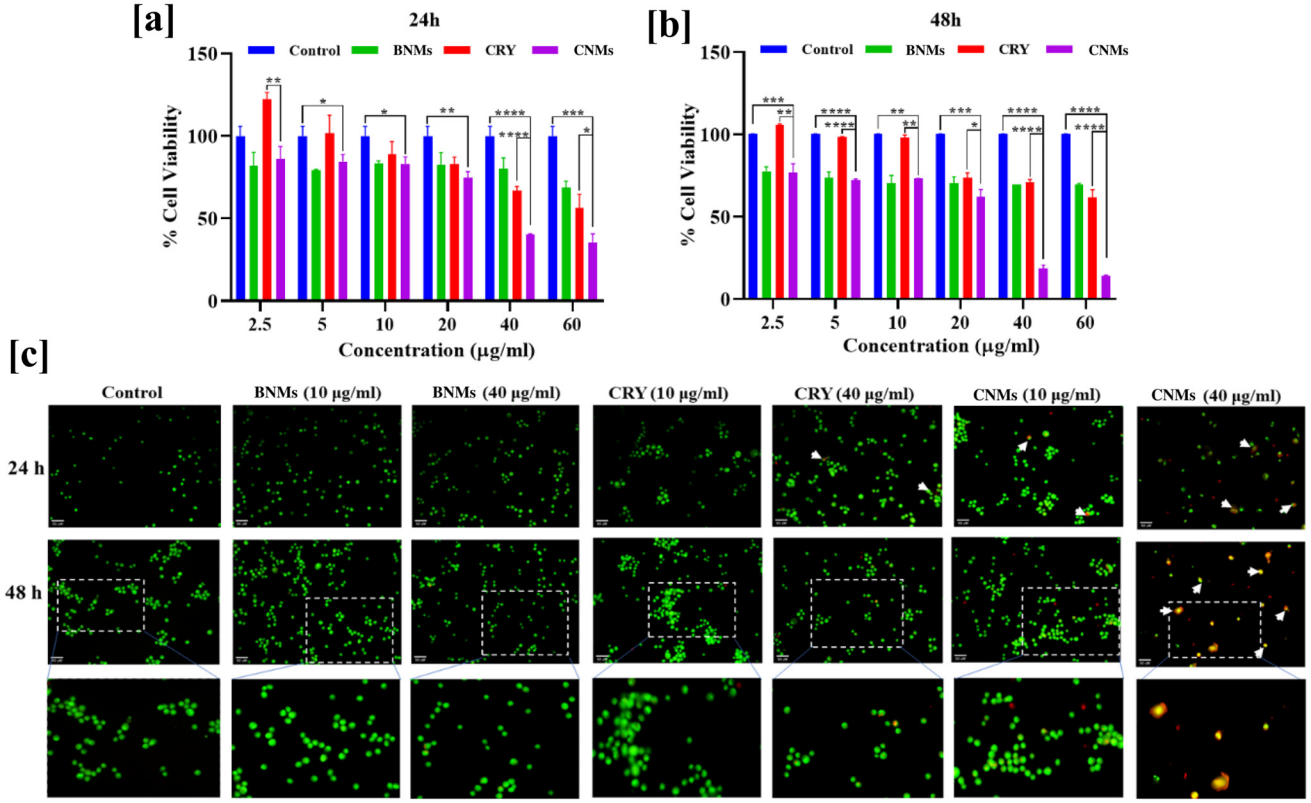

Fig. 4 (a and b) Effect of chrysin (CRY), genistein (GEN), blank PF68–SA nanomicelles (BNMs), chrysin-loaded PF68–SA nanomicelles (CNMs) and genistein-loaded PF68–SA nanomicelles (CNMs) on the viability of adenocarcinoma cell treatment at different concentrations and time intervals. Values represent mean ± SD (n = 3) where CNMs were found to significantly decrease the viable cell percentage as compared to control-untreated cells and CRY (* represents $p < 0.5$, ** represents $p < 0.01$, *** represents $p < 0.001$, and **** represents $p < 0.0001$) and the GNM-treated group of cells when compared to control- and GEN-treated cells (* represents $p < 0.5$, ** represents $p < 0.01$, *** represents $p < 0.001$ and **** represents $p < 0.0001$). (c) CNMs induce human A549 lung adenocarcinoma cell death: A549 cells after treatment with 10 and 40 µg mL^{-1} concentrations of CRY, BNMs, and CNMs were subjected to AO/EtBr staining at 24 and 48 h time points. The white enlarged boxes in the images depict early apoptotic cells with a green condensed or fragmented nucleus and orange late apoptotic cells with a condensed or fragmented nucleus. All the images were acquired on a Zeiss fluorescence microscope at 200× magnification.

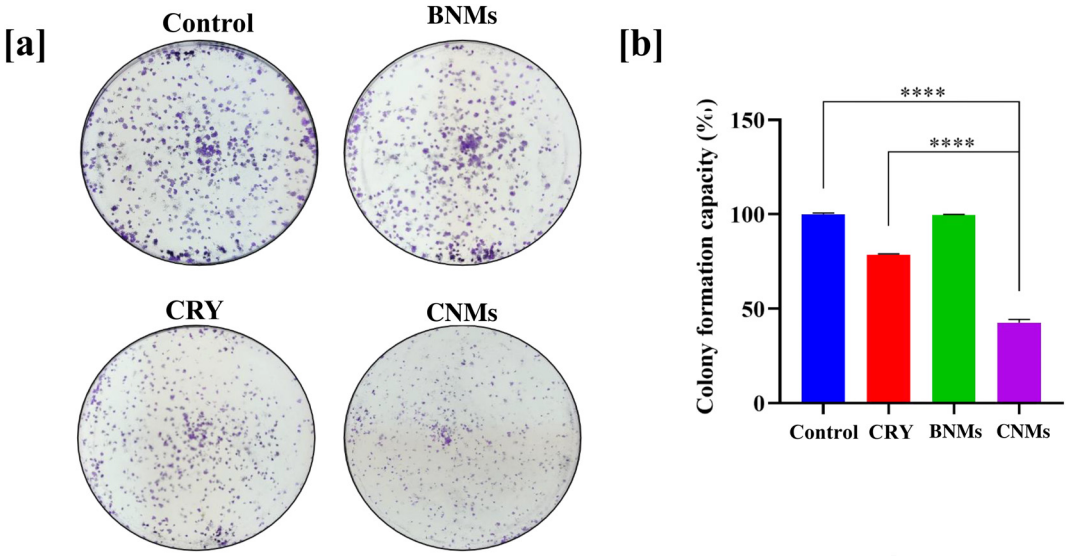

Fig. 5 Depiction of the long-term anticancer activity and reduced colony formation potential of (a) CRY, BNMs, and CNMs at 10 µg mL^{-1} on A549 cells. (b) Quantitative assessment of the percentage colony formation capacity of cells when compared to control-untreated cells (****$p < 0.0001$). Values represent mean ± SD (n = 3).

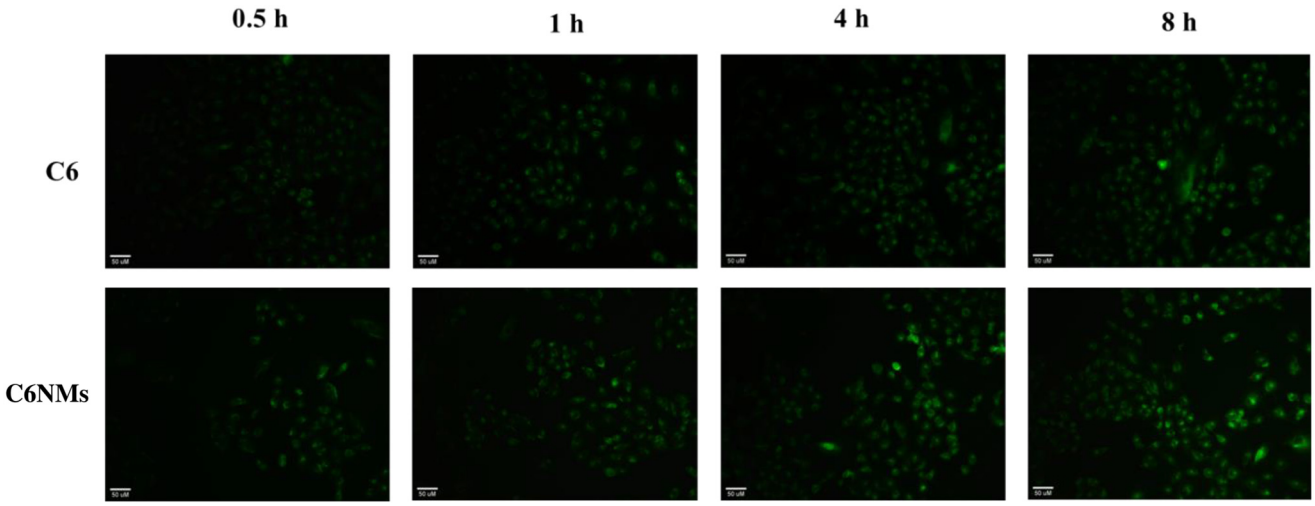

Fig. 6 Cellular uptake of the native fluorochrome, coumarin 6 (C6), and coumarin-loaded PF68–SA nanomicelles (C6NMs) in human adenocarcinoma A549 cells monitored at various time intervals. Images were captured using a fluorescence microscope (Zeiss) at 200× magnification.

cells had a significantly reduced colony formation potential (42.5%, $p < 0.0001$) compared to the control group. Additionally, as compared to bolus CRY, the CNMs, potentially, more significantly reduced the colony formation ability of A549 lung adenocarcinoma cells ($p < 0.0001$). The BNMs (10 μg mL^{-1}), being nontoxic to cells, did not impact the colony formation potential of cells, corroborating results from earlier experiments concerning their nontoxic attributes (Fig. 5). As a result, these observations clearly indicate that CNMs can arrest reproductive cell growth and significantly reduce the colony formation potential of lung A549 adenocarcinoma cells.

3.6 Cellular uptake of nanomicelles

The cellular uptake of nanomicelles is a critical aspect of their effectiveness as drug delivery systems. The cellular uptake of nanomicelles determines how effectively the encapsulated drug is delivered to its intended site of action and is assessed using a fluorescence microscope. However, CRY is a non-fluorescent molecule, and therefore we encapsulate the coumarin-6 (C6) in the PF68–SA biomaterial (C6NMs) and observed the cellular internalization of the nanomicelles using fluorescence analysis. The A549 cells were treated with the C6 suspension and C6NMs at 0.5, 1, 4 and 8 h. As illustrated in Fig. 6, the fluorescence intensity was higher in the cells incubated with CNMs. Compared to the C6 bolus the cells treated with CNMs started showing fluorescence from 1 h, which increased until 8 h, indicating the enhanced uptake of CNMs. C6-treated cells, however, showed an intense fluorescence intensity from 4 h onwards. These data confirm higher uptake of nanomicelles and correlate with the enhanced anticancer activity assessed earlier.

3.7 Nanomicelles enhanced the oral bioavailability of chrysin

An *in vivo* pharmacokinetics study of CNMs was conducted to assess the impact of the nanoformulation on the bioavailability of CRY. The plasma CRY concentration *versus* time profile for the CRY suspension and CNMs is presented in Fig. 7 and the main pharmacokinetics parameters are presented in Table 2. The results indicated that the maximum blood concentration (C_{max}) of the CNM formulation (2.84 μg mL^{-1}) was significantly higher than that of the CRY suspension (0.93 μg mL^{-1}). Similarly, the AUC_{0-t} of the CNMs was 5.6 times that of the CRY suspension, indicating that the relative bioavailability of the CRY was significantly improved due to

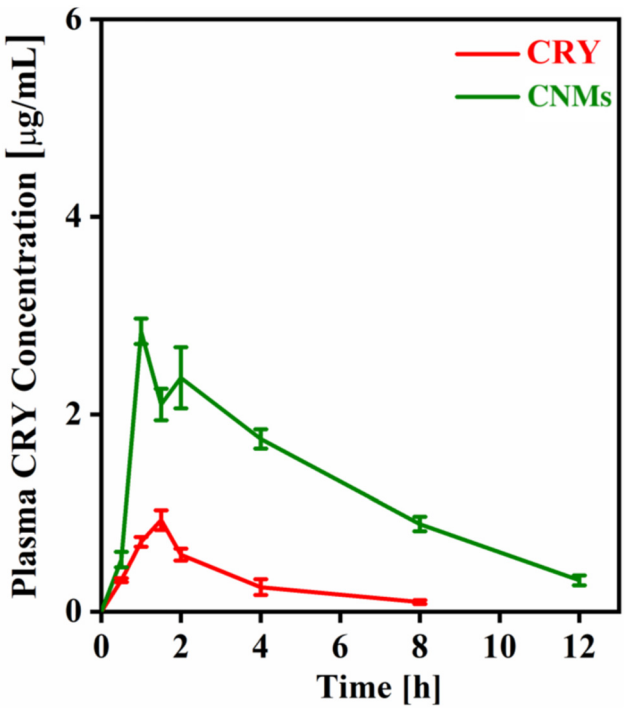

Fig. 7 The plasma concentration profile of chrysin (CRY) following the oral administration of the CRY suspension and chrysin-loaded nanomicelles (CNMs) evaluated in SD rats. Values represent mean ± SD (n = 6).

Table 2 Pharmacokinetics parameters of chrysin (CRY) and chrysin-loaded nanomicelles (CNMs). Values represent mean ± SD (n = 6)

Parameter	CRY	CNM	Unit
$t_{1/2}$	2.44 ± 0.3	3.49 ± 0.81	h
t_{max}	1.08 ± 0.34	1.75 ± 0.25	h
C_{max}	0.933 ± 0.18	2.84 ± 0.43	μg ml^{-1}
AUC_{0-t}	2.7 ± 0.69	15.1 ± 2.37	μg ml^{-1} h^{-1}
$MRT_{0\text{-inf\_obs}}$	3.74 ± 0.52	5.59 ± 1.24	h
$Cl/F_{\_obs}$	16.63 ± 2.79	2.98 ± 0.31	(mg kg^{-1}) (μg ml^{-1})$^{-1}$ h^{-1}

faster and enhanced absorption of CRY after administration as a nanomicelle formulation. The observed t_{max} values obtained at 1.08 h and 1.75 h for CNM and CRY suspensions, respectively, suggest the rapid absorption of CNMs. Furthermore, the mean residence time for the drug encapsulated in nanomicelles was also higher than the pure CRY, while its clearance was decreased 5.6 times.

4. Conclusion

In summary, the present study involved the fabrication of chrysin-loaded nanomicelles (CNMs) using a simple and cost-effective method. The CNMs exhibited a nanoparticle size distribution with spherical shapes. They also demonstrated sustained chrysin release profiles in upper gastrointestinal tract release media and long-term storage stability. Furthermore, the fabricated CNMs showed promising anticancer activity against human A549 lung cancer cells. The cell viability of CNMs was measured at 86% when administered at a concentration of 2.5 μg mL^{-1}. Subsequently, this decreased to 84.4%, 83%, 74.5%, 40.3%, and 35% after 24 hours of treatment. CNMs with a chrysin concentration of 40 μg mL^{-1} exhibited late apoptosis, with some cells displaying necrotic characteristics, appearing red with fragmented nuclei after 48 h of treatment. Moreover, the maximum blood concentration (C_{max}) and area under the curve (AUC_{0-t}) of the CNM formulation were found to be significantly higher than those of the bolus chrysin suspension. These observed results suggest the faster and enhanced absorption of chrysin after administration as a nanomicelle formulation.

Conflicts of interest

The authors declare that they have no known competing financial interests or personal relationships that could have appeared to influence the work reported in this paper.

Acknowledgements

HN and PPS would like to thank Bundelkhand University, Jhansi for providing necessary facilities and support. AKJ and HK acknowledge the Central University of Gujarat, Gandhinagar, and the Central Instrumental Facility (CIF-CUG) for providing the required resources and assistance.

References

1 M. Khasteband, Y. Sharifi and A. Akbari, Chrysin loaded polycaprolactone-chitosan electrospun nanofibers as potential antimicrobial wound dressing, *Int. J. Biol. Macromol.*, 2024, **263**, 130250, DOI: 10.1016/j.ijbiomac.2024.130250.
2 M. Yuce, M. Ekinci, M. Turan, G. Agar, M. Aydin, E. Ilhan and E. Yildirim, Chrysin mitigates copper stress by regulating antioxidant enzymes activity, plant nutrient and phytohormones content in pepper, *Sci. Hortic.*, 2024, **328**, 112887, DOI: 10.1016/j.scienta.2024.112887.
3 Y. Yi, R. Yu, H. Xue, Z. Jin, M. Zhang, Y. Bao, Z. Wang, H. Wei, X. Qiao and H. Yang, Chrysin 7-O-β-D-glucuronide, a dual inhibitor of SARS-CoV-2 3CL^{pro} and PL^{pro}, for the prevention and treatment of COVID-19, *Int. J. Antimicrob. Agents*, 2024, **63**, 107039, DOI: 10.1016/j.ijantimicag.2023.107039.
4 S. Güney, G. Yildiz, A. Capan and T. Ozturk, Evaluation of the electrochemical properties of 3-hydroxyflavone using voltammetric methods, *Electrochim. Acta*, 2010, **55**, 3295–3300, DOI: 10.1016/j.electacta.2009.12.078.
5 B. Y. Khoo, S. L. Chua and P. Balaram, Apoptotic Effects of Chrysin in Human Cancer Cell Lines, *Int. J. Mol. Sci.*, 2010, **11**(5), 2188–2199, DOI: 10.3390/ijms11052188.
6 G. Ozkan, T. Ceyhan, G. Çatalkaya, L. Rajan, H. Ullah, M. Daglia and E. Capanoglu, Encapsulated phenolic compounds: clinical efficacy of a novel delivery method, *Phytochem. Rev.*, 2024, DOI: 10.1007/s11101-023-09909-5.
7 U. Lesmes and D. J. McClements, Structure–function relationships to guide rational design and fabrication of particulate food delivery systems, *Trends Food Sci. Technol.*, 2009, **20**, 448–457, DOI: 10.1016/j.tifs.2009.05.006.
8 Z. Wang, X. Cheng, F. Meng, H. Guo, Z. Liu, H. Wang, J. Xu, H. Jin and L. Jiang, Wheat gliadin hydrolysates based nano-micelles for hydrophobic naringin: Structure characterization, interaction, and in vivo digestion, *Food Chem.: X*, 2024, **21**, 101136, DOI: 10.1016/j.fochx.2024.101136.
9 M.-L. Zhang, G.-P. Zhang, H.-S. Ma, Y.-Z. Pan and X.-L. Liao, Preparation of pH-responsive polyurethane nano micelles and their antibacterial application, *J. Biomater. Sci., Polym. Ed.*, 2024, **35**, 519–534, DOI: 10.1080/09205063.2024.2301807.
10 M. Malik, Z. Ali, S. Khan, A. Zeb, F. ud Din, A. H. Alamri and A. A. Lahiq, TPGS-PLA nanomicelles for targeting lung cancer; synthesis, characterization, and in vitro antitumor efficacy, *J. Drug Delivery Sci. Technol.*, 2024, **91**, 105238, DOI: 10.1016/j.jddst.2023.105238.
11 M. Bagheri-Meyabad, H. Motasadizadeh, P. Norouzi, Y. Fatahi, H. Asadi, R. Varshochian, M. Ghazi-Khansari and R. Dinarvand, Self-assembled NIPAM–PEG–NIPAM polymeric nanomicelles for the delivery of zinc protoporphyrin:

a potential stimuli-triggered cancer treatment approach, *J. Mater. Sci.*, 2024, **11**, 3049–3065, DOI: **10.1007/s10853-024-09410-0**.

12 E. A. Dalgakiran, A. D. Ergin and G. Kacar, Properties of Pluronic F68 and F127 micelles interacting furosemide from coarse-grained molecular simulations as validated by experiments, *Colloids Surf., A*, 2023, **666**, 131352, DOI: **10.1016/j.colsurfa.2023.131352**.

13 S. Shaarani, S. S. Hamid and N. H. Mohd Kaus, The Influence of Pluronic F68 and F127 Nanocarrier on Physicochemical Properties, In vitro Release, and Antiproliferative Activity of Thymoquinone Drug, *Pharmacogn. Res.*, 2017, **9**, 12–20, DOI: **10.4103/0974-8490.199774**.

14 T. T. C. Nguyen, C. K. Nguyen, T. H. Nguyen and N. Q. Tran, Highly lipophilic pluronics-conjugated polyamidoamine dendrimer nanocarriers as potential delivery system for hydrophobic drugs, *Mater. Sci. Eng., C*, 2017, **70**, 992–999, DOI: **10.1016/j.msec.2016.03.073**.

15 A. Besheer, J. Vogel, D. Glanz, J. Kressler, T. Groth and K. Mäder, Characterization of PLGA nanospheres stabilized with amphiphilic polymers: Hydrophobically modified hydroxyethyl starch vs pluronics, *Mol. Pharm.*, 2009, **6**, 407–415, DOI: **10.1021/mp800119h**.

16 Y. Song, Q. Tian, Z. Huang, D. Fan, Z. She, X. Liu, X. Cheng, B. Yu and Y. Deng, Self-assembled micelles of novel amphiphilic copolymer cholesterol-coupled F68 containing cabazitaxel as a drug delivery system, *Int. J. Nanomed.*, 2014, **9**, 2307–2317, DOI: **10.2147/IJN.S61220**.

17 Y. Cai, Z. Sun, X. Fang, X. Fang, F. Xiao, Y. Wang and M. Chen, Synthesis, characterization and anti-cancer activity of Pluronic F68–curcumin conjugate micelles, *Drug Delivery*, 2016, **23**, 2587–2595, DOI: **10.3109/10717544.2015.1037970**.

18 A. K. Jangid, K. Patel, P. Jain, S. Patel, N. Gupta, D. Pooja and H. Kulhari, Inulin-pluronic-stearic acid based double folded nanomicelles for pH-responsive delivery of resveratrol, *Carbohydr. Polym.*, 2020, **247**, 116730, DOI: **10.1016/j.carbpol.2020.116730**.

19 A. K. Jangid, H. Agraval, N. Gupta, U. C. S. Yadav, R. Sistla, D. Pooja and H. Kulhari, Designing of fatty acid-surfactant conjugate based nanomicelles of morin hydrate for simultaneously enhancing anticancer activity and oral bioavailability, *Colloids Surf., B*, 2019, **175**, 202–211, DOI: **10.1016/j.colsurfb.2018.11.073**.

20 A. K. Jangid, H. Agraval, D. B. Rai, P. Jain, U. C. Yadav, D. Pooja and H. Kulhari, Baicalin encapsulating lipid-surfactant conjugate based nanomicelles: Preparation, characterization and anticancer activity, *Chem. Phys. Lipids*, 2020, **233**, 104978, DOI: **10.1016/j.chemphyslip.2020.104978**.

21 A. K. Jangid, H. Agraval, N. Gupta, U. C. S. Yadav, R. Sistla, D. Pooja and H. Kulhari, Designing of fatty acid-surfactant conjugate based nanomicelles of morin hydrate for simultaneously enhancing anticancer activity and oral bioavailability, *Colloids Surf., B*, 2019, **175**, 202–211, DOI: **10.1016/j.colsurfb.2018.11.073**.

22 P. Yadav, C. Dua and A. Bajaj, Advances in Engineered Biomaterials Targeting Angiogenesis and Cell Proliferation for Cancer Therapy, *Chem. Rec.*, 2022, 202200152, DOI: **10.1002/tcr.202200152**.

23 J. Wang, H. Yang, Q. Li, X. Wu, G. Di, J. Fan, D. Wei and C. Guo, Novel nanomicelles based on rebaudioside A: A potential nanoplatform for oral delivery of honokiol with enhanced oral bioavailability and antitumor activity, *Int. J. Pharm.*, 2020, **590**, 119899, DOI: **10.1016/j.ijpharm.2020.119899**.

24 P. Muley, S. Kumar, F. El Kourati, S. S. Kesharwani and H. Tummala, Hydrophobically modified inulin as an amphiphilic carbohydrate polymer for micellar delivery of paclitaxel for intravenous route, *Int. J. Pharm.*, 2016, **500**, 32–41, DOI: **10.1016/j.ijpharm.2016.01.005**.

25 H. Cabral, K. Miyata, K. Osada and K. Kataoka, Block Copolymer Micelles in Nanomedicine Applications, *Chem. Rev.*, 2018, **118**, 6844–6892, DOI: **10.1021/acs.chemrev.8b00199**.

26 X. Li, M. Wang, C. Liu, X. Jing and Y. Huang, TAT-modified mixed micelles as biodegradable targeting and delivering system for cancer therapeutics, *J. Appl. Polym. Sci.*, 2013, **130**, 4598–4607, DOI: **10.1002/app.39744**.

27 L. Cheng, T. Luan, D. Liu, J. Cheng, H. Li, H. Wei, L. Zhang, J. Lan, Y. Liu and G. Zhao, Diblock copolymer glyco-nanomicelles constructed by a maltoheptaose-based amphiphile for reduction- and pH-mediated intracellular drug delivery, *Polym. Chem.*, 2018, **9**, 1337–1347, DOI: **10.1039/c7py01601h**.

28 D. Mandracchia, A. Rosato, A. Trapani, T. Chlapanidas, I. M. Montagner, S. Perteghella, C. Di Franco, M. L. Torre, G. Trapani and G. Tripodo, Design, synthesis and evaluation of biotin decorated inulin-based polymeric micelles as long-circulating nanocarriers for targeted drug delivery, *Nanomedicine*, 2017, **13**, 1245–1254, DOI: **10.1016/j.nano.2017.01.001**.

29 A. Mohan, S. V. Nair and V.-K. Lakshmanan, Polymeric nanomicelles for cancer theragnostics, *Int. J. Polym. Mater. Polym. Biomater.*, 2018, **67**, 119–130, DOI: **10.1080/00914037.2017.1309540**.

30 V. D. Samith, S. Navarro and R. Dabirian, Morphological and Semi-empirical Study of the Pluronic F68/Imogolite/Sudan III Intersurfaces Composite for the Controlled Temperature Release of Hydrophobic Drugs, *ACS Omega*, 2020, **5**, 20707–20723, DOI: **10.1021/acsomega.9b02965**.

31 X.-B. Fang, J.-M. Zhang, X. Xie, D. Liu, C.-W. He, J.-B. Wan and M.-W. Chen, pH-Sensitive micelles based on acid-labile Pluronic F68–curcumin conjugates for improved tumor intracellular drug delivery, *Int. J. Pharm.*, 2016, **502**, 28–37, DOI: **10.1016/j.ijpharm.2016.01.029**.

32 A. M. Bodratti and P. Alexandridis, Formulation of poloxamers for drug delivery, *J. Funct. Biomater.*, 2018, **9**, 11, DOI: **10.3390/jfb9010011**.

33 A. Bose, D. Roy Burman, B. Sikdar and P. Patra, Nanomicelles: Types, properties and applications in drug delivery, *IET Nanobiotechnol.*, 2021, **15**, 19–27, DOI: **10.1049/nbt2.12018**.

34 M. Callari, P. L. De Souza, A. Rawal and M. H. Stenzel, The Effect of Drug Loading on Micelle Properties: Solid-State NMR as a Tool to Gain Structural Insight, *Angew. Chem., Int. Ed.*, 2017, **56**, 8441–8445, DOI: **10.1002/anie.201701471**.

35 R. Pignatello, R. Corsaro, A. Bonaccorso, E. Zingale, C. Carbone and T. Musumeci, Soluplus® polymeric nanomicelles improve solubility of BCS-class II drugs, *Drug Delivery Transl. Res.*, 2022, **12**, 1991–2006, DOI: **10.1007/s13346-022-01182-x**.

36 R. Jog and D. J. Burgess, Pharmaceutical Amorphous Nanoparticles, *J. Pharm. Sci.*, 2017, **106**, 39–65, DOI: **10.1016/j.xphs.2016.09.014**.

37 X. Zhang, J. Li, R. Rong, D. Wang, D. Wang, Y. Yu, P. Wu, Y. Li and Z. Zhang, Enhancing the oral bioavailability of poorly water-soluble amisupiride with solid nanodispersion, *J. Drug Delivery Sci. Technol.*, 2023, **86**, 104635, DOI: **10.1016/j.jddst.2023.104635**.

38 L. Tang, L. Fu, Z. Zhu, Y. Yang, B. Sun, W. Shan and Z. Zhang, Modified mixed nanomicelles with collagen peptides enhanced oral absorption of cucurbitacin B: Preparation and evaluation, *Drug Delivery*, 2018, **25**, 862–871, DOI: **10.1080/10717544.2018.1425773**.

39 Y. K. Sung and S. W. Kim, Recent advances in polymeric drug delivery systems, *Biomater. Res.*, 2020, **24**, 12, DOI: **10.1186/s40824-020-00190-7**.

40 R. Kumar, A. Sirvi, S. Kaur, S. K. Samal, S. Roy and A. T. Sangamwar, Polymeric micelles based on amphiphilic oleic acid modified carboxymethyl chitosan for oral drug delivery of BCS class IV compound: Intestinal permeability and pharmacokinetic evaluation, *Eur. J. Pharm. Sci.*, 2020, **153**, 105466, DOI: **10.1016/j.ejps.2020.105466**.

41 S. K. Hari, A. Gauba, N. Shrivastava, R. M. Tripathi, S. K. Jain and A. K. Pandey, Polymeric micelles and cancer therapy: an ingenious multimodal tumor-targeted drug delivery system, *Drug Delivery Transl. Res.*, 2023, **13**, 135–163, DOI: **10.1007/s13346-022-01197-4**.

42 B. Ghosh and S. Biswas, Polymeric micelles in cancer therapy: State of the art, *J. Controlled Release*, 2021, **332**, 127–147, DOI: **10.1016/j.jconrel.2021.02.016**.

43 E. R. Kasala, L. N. Bodduluru, R. M. Madana, K. V. Athira, R. Gogoi and C. C. Barua, Chemopreventive and therapeutic potential of chrysin in cancer: mechanistic perspectives, *Toxicol. Lett.*, 2015, **233**, 214–225, DOI: **10.1016/j.toxlet.2015.01.008**.

44 A. Eatemadi, H. Daraee, H. T. Aiyelabegan, B. Negahdari, B. Rajeian and N. Zarghami, Synthesis and Characterization of Chrysin-loaded PCL-PEG-PCL nanoparticle and its effect on breast cancer cell line, *Biomed. Pharmacother.*, 2016, **84**, 1915–1922, DOI: **10.1016/j.biopha.2016.10.095**.